Low-Energy Near-Earth Asteroid Capture using Momentum Exchange Strategies

Minghu Tan*, Colin R. McInnes†, Matteo Ceriotti‡
University of Glasgow, Glasgow G12 8QQ, United Kingdom

This paper investigates the concept of capturing small near-Earth asteroids into bound periodic orbits at the Sun-Earth L_1 and L_2 points using momentum exchange. A small asteroid is first maneuvered to engineer a fly-by with a larger asteroid. Two strategies are then considered: when the small asteroid approaches the vicinity of the large asteroid, it will either impact the large asteroid or connect to it with a tether. In both strategies, momentum exchange can be used to effect the capture of one of the asteroids. Then, a two-impulse Lambert arc is utilized to design a post-encounter transfer trajectory to the stable manifolds of the Sun-Earth L_1 or L_2 points. A selection strategy for candidate asteroids is proposed by considering both the deflection windows for capturing asteroids and the size of the asteroids. By investigating the outcome of the impact on the small asteroid, or the tension of the tether, the maximum velocity increment available using these momentum exchange strategies is investigated. Finally, a detailed design procedure is presented which is then optimized using a global optimization strategy. The results show that, in principle, capture strategies using momentum exchange have the potential to deliver low-energy capture of asteroids although significant practical challenges remain.

Nomenclature

A = constant cross-sectional area, m^2

D = asteroid diameter, m

E = impact kinetic energy, erg

H = asteroid absolute magnitude

* Ph.D. Candidate, School of Engineering, James Watt South Building; m.tan.2@research.gla.ac.uk.
† James Watt Chair, Professor, School of Engineering, James Watt South Building; colin.mcinnes@glasgow.ac.uk.
‡ Lecturer, School of Engineering, James Watt South Building; matteo.ceriotti@glasgow.ac.uk. Member AIAA.

J = Jacobi constant

k = coefficient of restitution

L = tether length, m

m_l = mass of large asteroid, kg

m_s = mass of small asteroid, kg

m_{tether} = mass of tether, kg

$\boldsymbol{n}$ = unit normal vector along the mass centers of the asteroids

$\boldsymbol{O}_l$ = center-of-mass of large asteroid

$\boldsymbol{O}_s$ = center-of-mass of small asteroid

p_v = asteroid albedo

S_0 = maximum safe working stress, GPa

S_{s0} = material impact strength of small asteroid, J/m^3

S_s = effective impact strength of small asteroid, J/m^3

S = tether stress, GPa

T_L = tether tension at the small asteroid

v_c = characteristic velocity of the tether material, m/s

$\boldsymbol{v}_{l-}$ = velocity vector of the large asteroid before impact or tether-assisted flyby, m/s

$\boldsymbol{v}_{l+}$ = velocity vector of the large asteroid after impact or tether-assisted flyby, m/s

$\boldsymbol{v}_{s-}$ = velocity vector of small asteroid before impact or tether-assisted flyby, m/s

$\boldsymbol{v}_{s+}$ = velocity vector of small asteroid after impact or tether-assisted flyby, m/s

$\boldsymbol{v}_{sl}$ = relative velocity of small asteroid with respect to the large asteroid, m/s

$\Delta v_{2\min}$ = minimum value of the second impulse, m/s

$\Delta \boldsymbol{v}_n$ = relative velocity between the two asteroids in direction $\boldsymbol{n}$, m/s

$\Delta \boldsymbol{v}_{release}$ = relative velocity of small asteroid with respect to the large asteroid when released, m/s

$\Delta v_{threshold}$ = threshold value of $\Delta \boldsymbol{v}_n$, m/s

Δv = total cost, m/s

μ = non-dimensional mass parameter of the Earth and Sun

ρ = asteroid density, kg/m^3

ρ_{tether} = tether density, kg/m^3

$\boldsymbol{\tau}$ = unit tangent vector

Subscripts

l = large asteroid

s = small asteroid

I. Introduction

NEAR Earth Asteroids offers both a threat and an opportunity. On one hand, they represent a (small) potential threat due to planetary impact resulting in regional or global disaster. On the other hand, they also offer abundant resources to support the long-term human exploration of space and the future development of the solar system.

Near Earth asteroids typically have orbits that lie partly between 0.983 and 1.3 AU from the Sun [1]. Therefore, they present the closest potential threats for Earth impact and the easiest targets both to reach from the Earth and to capture at the Earth. To capture asteroids with low energy, Yárnoz et al. [2] recently identified a new family of asteroids, termed easily retrievable objects. Easily retrievable objects are asteroids which can be gravitationally captured into bound periodic orbits around the Sun-Earth L_1 and L_2 points with a total cost of less than 500 m/s. A two impulsive Lambert arc was utilized to design the transfer trajectory from the candidate easily retrievable object's initial orbit to the stable manifold associated with the target periodic orbit. Furthermore, Mingotti et al. [3] employed low thrust to capture easily retrievable objects into periodic orbits around the Sun-Earth L_1 and L_2 points. Moreover, Sánchez and Yárnoz [4] updated the list of easily retrievable objects and estimated the largest retrievable mass possible to investigate the feasibility of asteroid resource utilization. As the catalogue of asteroids is updated with further observations, it is likely that more easily retrievable objects will be found in the future.

The Earth-Moon L_1 and L_2 points have been regarded as two of the preferred positions to place captured asteroids. This is because spacecraft in vicinity of the Earth-Moon L_1 and L_2 points can easily reach the Moon, Earth and Sun-Earth L_1 and L_2 points. Moreover, if a mission capturing asteroids at the Earth-Moon L_1 or L_2 points fails, the captured asteroid would possibly impact the Moon and thus may reduce the probability of asteroid impact with the Earth [5]. NASA has proposed a near-Earth asteroid retrieval mission to capture an asteroid, or part of an asteroid, and place it in a lunar distant retrograde orbit [5, 6]. The bi-circular restricted three-body problem model,

which couples together the Sun–Earth and Earth–Moon circular restricted three-body problems, has been used to investigate the capture of asteroids into periodic orbits in the Earth–Moon system [7]. Among the asteroids, the temporarily captured asteroids have also been regarded as attractive candidates for the near-Earth asteroid retrieval mission [8].

Momentum exchange theory can be used as a strategy to achieve maneuvers or redirect target bodies by transporting the momentum from one object to the target [9, 10]. Generally speaking, this technique can be classified into instantaneous momentum exchange and slow momentum exchange techniques. Slow momentum exchange techniques can provide continuous maneuvers and has been studied extensively for asteroid deflection using the gravity tractor or ion-beam shepherding [11-13]. One the other hand, instantaneous momentum exchange is usually utilized to generate a single impulse and has also been widely applied to research on asteroids, including asteroid deflection by impactors and tether-assist [14-18]. In this paper, we only focus on the instantaneous momentum exchange technique. Among the many deflection techniques, the kinetic impactor appears to be feasible with current technology. In this deflection strategy, a spacecraft with a kinetic impactor is first guided to directly impact a target asteroid at a sufficiently high velocity such that the momentum of the impactor is transferred to the target asteroid, causing a modification of the target asteroid's orbit with respect to its unperturbed orbit. In fact, only a modest perturbation to the target asteroid's original orbit is sufficient to achieve desired useful deflections, provided that the warning time is sufficiently long [15]. However, if the warning time is short, a large momentum transfer is required. A means of improving momentum transfer through engineering a 'billiard shot' asteroid collision has been proposed by Canavan and Rather [19]. The key idea of this method is to use a small asteroid to impact a large asteroid for deflection. In this deflection strategy, a spacecraft is first guided to impact on a small asteroid, which is then delivered to approach a large target asteroid. The trajectory of the large target asteroid is then deflected through collision with the small asteroid. Furthermore, a way of improving the efficiency of this deflection strategy has been proposed [20], through placing the small asteroid onto an Earth swing-by trajectory to modify the trajectory of the small asteroid and hence enhance the resulting momentum transfer. Because the mass of the small asteroid is much larger than that of the spacecraft, this deflection method can in principle leverage more efficient asteroid deflection strategies. It should be noted that this method requires an accurate dynamical model of the orbits and properties of the relevant bodies, and there must be a small asteroid in the database with the appropriate orbital elements and size.

The classical gravity assist method has been studied extensively and is regarded as a basic tool for the design of low-energy interplanetary transfer trajectories [21]. Between entering and leaving the gravitational field of a planet, a spacecraft's heliocentric velocity can change significantly. An example of the classical gravity assist is to investigate the accessibility of main-belt asteroids [22]. However, due to their weak gravitational field, asteroids are not suitable for such maneuvers. Nevertheless, Penzo and Mayer [17] proposed the use of a tether to temporarily connect a spacecraft with an asteroid for a tethered fly-by maneuver. During the tethered flyby, the spacecraft is assumed to be attached to the asteroid with a tether, such that the spacecraft can swing around the asteroid through a large angle to yield a similar velocity change as a gravity assist from a planet or moon. Such tether dynamics were also utilized to study the possibility of tethering two asteroids, in order to capture one of them for resource extraction [18]. A similar idea of connecting a spacecraft to a moon in the circular restricted three-body problem has been proposed to achieve subsequent capture of the spacecraft by the planet [23]

In this paper, momentum exchange theory, including both kinetic impacts and the use of tethered assist is applied to the capture of small asteroids into periodic orbits around the Sun-Earth L_1 and L_2 points. In the first capture strategy using kinetic impacts, the small asteroid leaves its initial orbit through an impulse delivered from a spacecraft and then approaches a large target asteroid. Accordingly, the small asteroid then collides with the large asteroid with an impact geometry such that the small asteroid will be captured onto the stable manifold associated with the Sun-Earth L_1 or L_2 points, thus leveraging the orbit energy of the large asteroid. In the capture strategy using the tethered assist, after a targeting impulse, the small asteroid approaches the large asteroid and then connects with the large asteroid through a tether; the tether is then released after the flyby maneuver. As a result, the small asteroid will again be transferred onto the stable manifold associated with the Sun-Earth L_1 or L_2 points. The key contributions of the paper are therefore in coupling momentum exchange strategies to invariant manifolds, dynamical models of the kinetic impact and the tether-assisted flyby. The paper then investigates optimizing these strategies to achieve low-energy capture of the small asteroid onto periodic orbits around the Sun-Earth L_1 or L_2 points.

The present paper is organized as follows. Section II presents the dynamical model of the circular restricted three-body problem, periodic orbits and the invariant manifolds; Section III studies the characteristics of the asteroids, including their mass, deflection windows and a list of candidate asteroids; Section IV describes the

detailed designed procedure of capturing small asteroids by impacting with large asteroids; finally, Section V studies the design procedure of asteroid capture using the tethered assist strategy.

II. Dynamical model

In both asteroid capture strategies using momentum exchange, the small asteroid leaves its orbit and will be inserted onto the stable manifold associated with the periodic orbits of the Sun-Earth L_1 or L_2 points after the momentum exchange encounter. During the transfer from the asteroid orbit to the stable manifold, the motion of the asteroid is considered in the Sun-asteroid two-body problem. When the small asteroid is captured onto the stable manifold, it will then be modelled by the Sun-Earth circular restricted three-body problem.

A. Circular restricted three-body problem

The motion of the asteroid (of negligible mass) is investigated in the gravitational field generated by two primary bodies, the Sun and Earth. Assuming that the Sun and Earth are in a circular orbit about their common center-of-mass, the dynamical model of the circular restricted three-body problem, centered at the barycenter, can be written as [24]

$$\ddot{x} - 2\dot{y} = \frac{\partial \Omega}{\partial x}, \ddot{y} + 2\dot{x} = \frac{\partial \Omega}{\partial y}, \ddot{z} = \frac{\partial \Omega}{\partial z} \tag{1}$$

where

$$\Omega(x, y, z, \mu) = \frac{1}{2}(x^2 + y^2) + \frac{1-\mu}{r_1} + \frac{\mu}{r_2}$$

The three-body mass ratio μ is assumed for this model to be $\mu = 3.036 \times 10^{-6}$ [24] and $r_1 = [(x+\mu)^2 + y^2 + z^2]^{1/2}$, $r_2 = [(x-1+\mu)^2 + y^2 + z^2]^{1/2}$ are the magnitudes of the position vectors to the two primary bodies, scaled by the distance between the Sun and Earth (Astronomical Unit, AU).

The Jacobi constant J is then defined as [25]

$$J = 2\Omega(x, y, z, \mu) - (\dot{x}^2 + \dot{y}^2 + \dot{z}^2) \tag{2}$$

Moreover, there are five well-known equilibrium points in the circular restricted three-body problem, the Lagrange points or libration points, L_i, (i = 1, …, 5). In this paper, L_1 and L_2 are the target libration points for the captured asteroids.

B. Periodic orbits and invariant manifolds

Due to the many potential applications of space missions in near-Earth space, periodic orbits around the collinear libration points have generated significant interest in recent years and have been studied extensively by many researchers [26-30]. Families of the periodic orbits exist in both two and three-dimensions, corresponding to the two common classifications of periodic orbits: halo orbits and Lyapunov orbits. One class of periodic orbits chosen for this work is the family of Lyapunov orbits. Based on the third-order Richardson expansion of periodic orbits [28], the accurate initial state of a small Lyapunov orbit can be calculated through a numerical procedure, based on perturbation techniques, in order to correct the initial analytic estimates provided by the third-order expansion. Then the accurate initial state of the Lyapunov orbit is utilized as an initial guess for a new Lyapunov obit which can be calculated using differential correction with a slightly larger displacement in the amplitude in x-axis. Accordingly, this process can be repeated and thus families of Lyapunov orbits can be calculated by decreasing or increasing the associated Jacobi constant, as shown in Fig. 1.

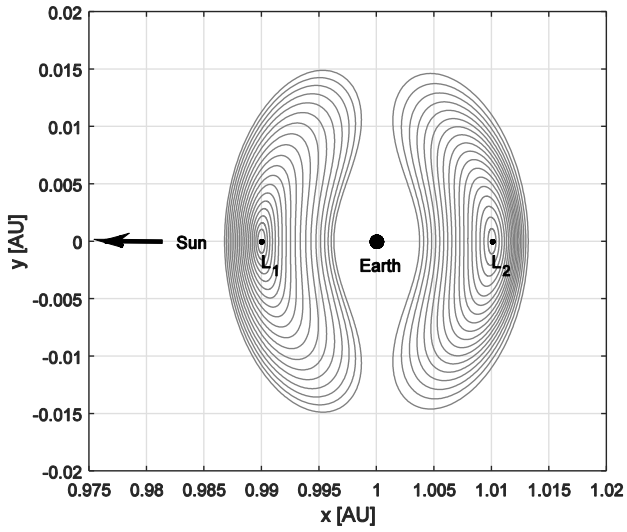

Fig. 1 Lyapunov orbits with Jacobi constant [3.00006018, 3.00089706] around the Sun-Earth L_1 point and Lyapunov orbits with Jacobi constant [3.00023977, 3.00089301] around the Sun-Earth L_2 point.

Invariant manifolds associated with periodic orbits around the collinear libration points are key to the design of low-energy transfer trajectories [26, 27]. According to their different dynamical characteristics, the invariant manifolds can be classified as stable manifolds (W^S) and unstable manifolds (W^U). The stable manifolds associated with a periodic orbit contain all possible trajectories which asymptotically approach the target periodic orbit. The unstable manifold consists of the set of trajectories that asymptotically depart from the target periodic orbit.

The Poincaré surface of section is now defined by a plane in position space $y = (x + \mu)\tan\beta$ where β is the angle of the section with respect to the Sun in the rotating frame, shown in Fig. 2. Transfer trajectories from the initial asteroid orbit to the stable manifolds associated with the Sun-Earth L_1 and L_2 periodic orbits can then be designed by solving for a Lambert arc in the two-body Sun-asteroid model. Here we set $\beta = \pm\pi/8$ as the threshold of the boundary of the Sun-asteroid two-body problem and the Sun-Earth circular restricted three-body problem ($\pi/8$ for the L_2 stable manifolds and $-\pi/8$ for the L_1 stable manifolds) [2, 4].

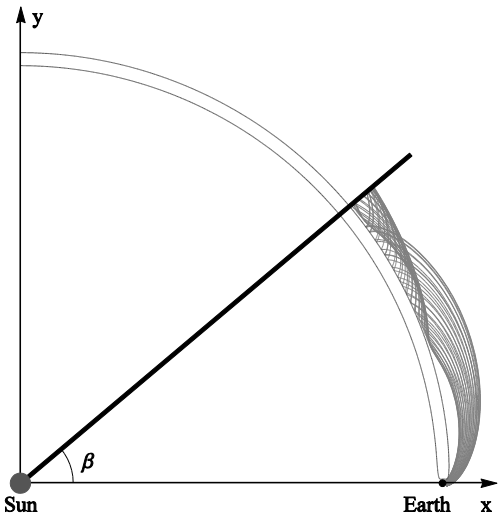

Fig. 2 Stable manifolds associated with the Lyapunov orbit around Sun-Earth L_2.

III. Characteristics of near-Earth asteroids

For the calculation of potential asteroid capture opportunities, the asteroid sample used for the analysis is the JPL Small-Body Database[§]. The database represents the known, catalogued asteroids including orbital elements and absolute magnitude.

[§]Data available at https://ssd.jpl.nasa.gov/?sb_elem

A. Mass of asteroids

Due to absence of information on their size, shape, and density, the mass of an asteroid is typically not known. In general, the only information available is the absolute magnitude H of the asteroid, a parameter associated with its intrinsic brightness. If we assume that the near-Earth asteroid is a homogeneous sphere with density ρ and diameter D, the mass of the asteroid is given by [31]

$$M = \frac{\pi}{6}\rho D^3 \tag{3}$$

The diameter of an asteroid (D) can also be estimated from its absolute magnitude (H), such that [31]

$$D = 1329\text{km} \times 10^{-H/5} p_v^{-1/2} \tag{4}$$

The lower the value of H, the larger the size of the asteroid. However, Eq. (4) also requires that the asteroid's albedo p_v is known. Since the albedo for most asteroids is unknown, the albedo range is usually assumed to be between 0.05 and 0.25. Here we assume that $p_v = 0.154$ [31].

B. Deflection windows

For a small candidate asteroid, feasible capture transfers will be obtained in the date interval 2020-2100 with the first synodic period of the asteroid considered. The orbital elements of the asteroids are also assumed to be valid until their next close encounter with the Earth. To clarify how close approaches can affect the orbital elements of the asteroids, we select 0.4 AU as a threshold distance between the Earth and asteroid, approximately corresponding to the threshold $\beta = \pm\pi/8$ in Section II.B. Beyond this distance, the gravitational influence of the Earth is considered to be small. Once the distance between the Earth and the asteroid is less than 0.4 AU, the orbital elements of the asteroid will be assumed to change. Thus, we define the date when the distance between the Earth and the asteroid is 0.4 AU as a threshold date. Given one small asteroid and one large asteroid, the threshold dates of the small asteroid and the large asteroid are denoted as T_s and T_l, respectively. Therefore, the domain of the impulse date (T_0) to deflect the small asteroid from its natural orbit and the flight time (T_{fly1}) from the impulse to the interception of the large asteroid should be

$$T_0 \in [2020, T_s], T_0 + T_{fly1} \in [2020, T_l] \tag{5}$$

C. Candidate asteroid filter

Potentially Hazardous Asteroids (PHAs) are those asteroids with an Earth Minimum Orbit Intersection Distance (MOID) of 0.05 AU or less and an absolute magnitude (H) of 22.0 or less [32]. PHAs can be considered to pose a potential threat to the Earth when they have a close approach. A momentum exchange encounter with an asteroid with H smaller than 22.0 but MOID larger than 0.05 AU may decrease the MOID and thus the asteroid may become a PHA. Therefore, asteroids with H smaller than 22.0 are unsuitable targets for momentum exchange. This is used as a filter criteria for the large asteroid so that candidate large asteroids should have $H > 22.0$.

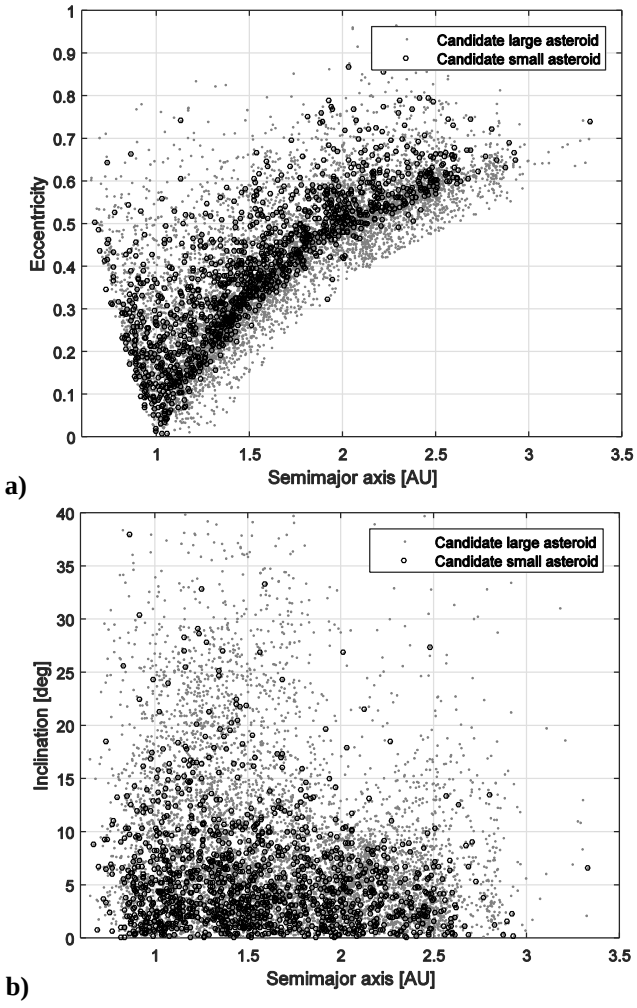

Fig. 3 Distribution of candidate large and small asteroids.

Furthermore, we set $D \leq 40$ m ($H \geq 24.7$) as a threshold on asteroid size since captured asteroids may also be a potential impact threat to Earth. Objects of 40 m in diameter can be considered as the critical threshold above which the Earth's atmosphere will no longer disintegrate the object [15]. Considering this filter criteria, the candidate small asteroids should therefore have $H \geq 24.7$.

In order to minimize the influence of the impact on the large asteroid, and so guarantee that the large asteroid orbit is almost unchanged before and after the encounter, we expect the mass of the large asteroid should be at least two orders of magnitude greater than that of the small asteroid such that

$$\frac{m_l}{m_s} \geq 100 \tag{6}$$

Considering a large asteroid with $H > 22$ and a mass ratio of the two asteroids as defined in Eq. (6), the small asteroid should be selected such that $H > 25.33$. All candidate large asteroids and small asteroids are shown in Fig. 3.

IV. Small asteroid capture through impact of a large asteroid

In this section, kinetic impact theory is applied to the capture of asteroids. In this capture strategy, the small asteroid leaves its initial orbit through an impulse from a spacecraft and then approaches a large target asteroid. At interception, the small asteroid collides with the large asteroid with impact geometry such that the small asteroid is deflected, and subsequently captured onto the stable manifold associated with the Sun-Earth L_1 or L_2 points, thus leveraging the orbit energy of the large asteroid.

A. Problem statement

Figure 4 shows an overview of the strategy for capturing a small asteroid by the impact of a large asteroid. The mission scenario consists of the following steps: with the first impulse $\Delta\boldsymbol{v}_1$, the small asteroid leaves its orbit and will approach the vicinity of the target large asteroid; then the small asteroid collides with the large asteroid and immediately after collision a second impulse $\Delta\boldsymbol{v}_2$ is required for a Lambert arc to intersect the stable manifold associated with the Sun-Earth L_1 or L_2 point; with the third impulse $\Delta\boldsymbol{v}_3$, the small asteroid is captured onto the stable manifold associated with the Sun-Earth L_1 or L_2 point.

Given one small asteroid and one large asteroid, there are 6 variables in the solution space: the date (T_0) of the first impulse $\Delta\boldsymbol{v}_1$, the flight time (T_{fly1}) of the small asteroid between the first impulse and the impact, the flight time (T_{fly2}) of the small asteroid between the collision and the impulse $\Delta\boldsymbol{v}_3$ for insertion onto the stable manifold, the Jacobi constant (J) of the target periodic orbit around the Sun-Earth L_1 or L_2 point, the parameter (t_p) determining the point on the periodic orbit where the stable manifold is calculated from, and the stable manifold transfer time (t_m) determining the point on the stable manifold where the small asteroid inserts onto it.

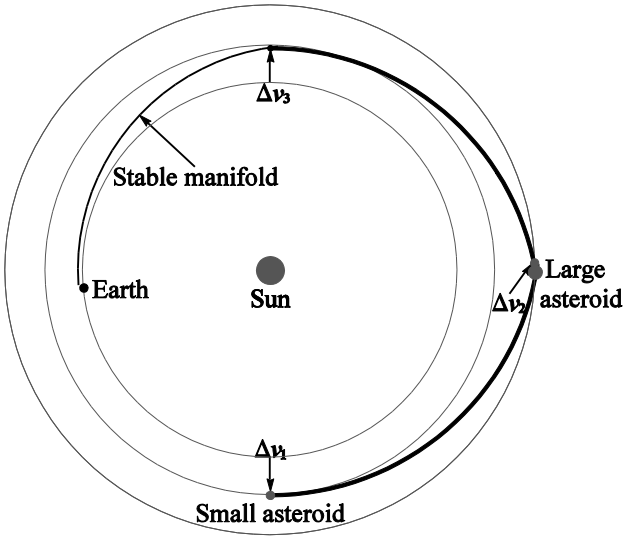

Fig. 4 Overview of small asteroid capture through impact of a large asteroid.

B. Collision geometry

In practice, the small asteroid needs to accurately target an impact point on the large asteroid. Moreover, the masses of the two asteroids and the momentum exchange parameter between the asteroids are major uncertainties. Therefore, high-precision navigation and pre-launch characterization and identification of the asteroid properties are necessary. We note that such uncertainties are clearly important, but we do not consider them in this paper whose aim is to define the overall capture strategy.

The collision geometry of a small asteroid with a large asteroid is shown schematically in Fig. 5. The unit normal vector $\boldsymbol{n}$ is along the center-of-mass of the two asteroids and the unit tangent vector $\boldsymbol{\tau}$ is perpendicular to $\boldsymbol{n}$. It will be assumed that the collision point is on the line $\boldsymbol{n}$ along the mass centers of the two asteroids and so we only consider the dynamics of the two asteroids in the direction of $\boldsymbol{n}$. According to the conservation of linear momentum, the velocity of the small asteroid after collision is given by [33]

$$\begin{cases} \boldsymbol{v}_{s\tau+} = \boldsymbol{v}_{s\tau-} \\ \boldsymbol{v}_{sn+} = \boldsymbol{v}_{sn-} - (1+k)\dfrac{m_l}{m_l + m_s}(\boldsymbol{v}_{sn-} - \boldsymbol{v}_{ln-}) \end{cases} \tag{7}$$

where $\boldsymbol{v}_{s\tau+} = (\boldsymbol{v}_{s+}{}^T\boldsymbol{\tau})\boldsymbol{\tau}$, $\boldsymbol{v}_{s\tau-} = (\boldsymbol{v}_{s-}{}^T\boldsymbol{\tau})\boldsymbol{\tau}$, $\boldsymbol{v}_{sn+} = (\boldsymbol{v}_{s+}{}^T\boldsymbol{n})\boldsymbol{n}$ and $\boldsymbol{v}_{sn-} = (\boldsymbol{v}_{s-}{}^T\boldsymbol{n})\boldsymbol{n}$.

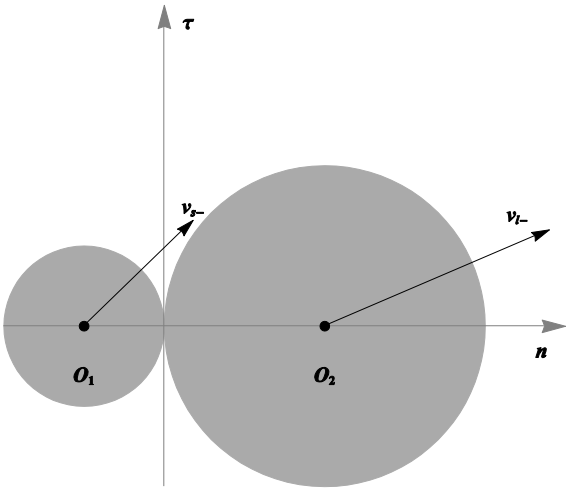

Fig. 5 Collision geometry of the two asteroids.

Therefore, Eq. (7) can be written as

$$\boldsymbol{v}_{s+} = \boldsymbol{v}_{s-} - (1+k)\frac{m_l}{m_l + m_s}((\boldsymbol{v}_{s-} - \boldsymbol{v}_{l-})^T \boldsymbol{n})\boldsymbol{n} \tag{8}$$

where the coefficient of restitution k is assumed to be 1 for a perfectly elastic collision. The relative velocity between the two asteroids in direction $\boldsymbol{n}$ can then be written as

$$\Delta v_n = \left|\Delta \boldsymbol{v}_{\boldsymbol{n}}\right| = \left|(\boldsymbol{v}_{s-} - \boldsymbol{v}_{l-})^T \boldsymbol{n}\right| \tag{9}$$

This relative velocity is key to estimating whether the small asteroid will remain intact or not after the collision. Here we denote $\Delta v_{threshold}$ as the threshold such that once $\Delta v_n > \Delta v_{threshold}$, disruption of the asteroid will occur, as will be discussed later. Assuming $\boldsymbol{v}_{Lam}$ is the required post-collision velocity vector of the small NEA obtained by solving the Lambert arc from the large NEA orbit to the stable manifold associated with Sun-Earth L_1 and L_2 periodic orbits, the second impulse $\Delta \boldsymbol{v}_2$ can therefore be written as

$$\Delta \boldsymbol{v}_2 = \boldsymbol{v}_{Lam} - \boldsymbol{v}_{s+} = \Delta \boldsymbol{v}_- - \lambda(\Delta \boldsymbol{v}_{ls}{}^T \boldsymbol{n})\boldsymbol{n} \tag{10}$$

where

$$\Delta \boldsymbol{v}_- = \boldsymbol{v}_{Lam} - \boldsymbol{v}_{s-}, \lambda = (1+k)\frac{m_l}{m_l + m_s}, \Delta \boldsymbol{v}_{ls} = \boldsymbol{v}_{l-} - \boldsymbol{v}_{s-}$$

Once the 6 variables (T_0, T_{fly1}, T_{fly2}, J, t_p, t_m) have been selected, the first impulse $\Delta\boldsymbol{v}_1$ and the third impulse $\Delta\boldsymbol{v}_3$ can then be determined by solving two Lambert arc problems, where the second impulse $\Delta\boldsymbol{v}_2$ is a function of the unit vector $\boldsymbol{n}$. The optimization problem can therefore be written as,

$$\begin{cases} \min \ \left|\Delta\boldsymbol{v}_2\right| \\ \left|\Delta\boldsymbol{v}_{ls}{}^T\boldsymbol{n}\right| < \Delta v_{threshold} \end{cases} \tag{11}$$

It should be noted that the set $(\lambda\Delta\boldsymbol{v}_{ls}{}^T\boldsymbol{n})\boldsymbol{n}$ is a sphere with diameter $\left|\lambda\Delta\boldsymbol{v}_{ls}\right|$ which is centered at $\frac{1}{2}\lambda\Delta\boldsymbol{v}_{ls}$. According to the geometric relationship between the vectors in Eq. (10), shown in Fig.6, there exists a critical value of $\boldsymbol{n}$, $\boldsymbol{n}_c = \dfrac{2\Delta\boldsymbol{v}_- + (1-\gamma)\lambda\Delta\boldsymbol{v}_{ls}}{\left|2\Delta\boldsymbol{v}_- + (1-\gamma)\lambda\Delta\boldsymbol{v}_{ls}\right|}$ where $\gamma = \dfrac{\left|\lambda\Delta\boldsymbol{v}_{ls}\right|}{\left|2\Delta\boldsymbol{v}_- - \lambda\Delta\boldsymbol{v}_{ls}\right|}$. When $\left|\Delta\boldsymbol{v}_{ls}{}^T\boldsymbol{n}_c\right| \le \Delta v_{threshold}$, shown in Fig. 6(a), the second impulse is minimized by choosing $\boldsymbol{n} = \boldsymbol{n}_c$ and this minimum value is found to be

$$\Delta v_{2\min} = \min(\left|\Delta\boldsymbol{v}_2\right|) = \frac{1}{2}\left|\left|2\Delta\boldsymbol{v}_- - \lambda\Delta\boldsymbol{v}_{ls}\right| - \left|\lambda\Delta\boldsymbol{v}_{ls}\right|\right| \tag{12}$$

On the other hand, if $\left|\Delta\boldsymbol{v}_{ls}{}^T\boldsymbol{n}_c\right| > \Delta v_{threshold}$, shown in Fig. 6(b), the second impulse is minimized when $\left|\Delta\boldsymbol{v}_{ls}{}^T\boldsymbol{n}\right| = \Delta v_{threshold}$ and the minimum value is then found to be

$$\Delta v_{2\min} = \min(\left|\Delta\boldsymbol{v}_2\right|) = \sqrt{p_2{}^2 + (\sqrt{p_1{}^2 - p_2{}^2} - p_3)^2} \tag{13}$$

where

$$\boldsymbol{X} = \frac{\lambda\Delta v_{threshold}{}^2}{\left|\Delta\boldsymbol{v}_{ls}\right|^2}\Delta\boldsymbol{v}_{ls},\ p_1 = \left|\Delta\boldsymbol{v}_- - \boldsymbol{X}\right|,\ p_2 = \left|\frac{\Delta\boldsymbol{v}_-{}^T\cdot\boldsymbol{X}}{\left|\boldsymbol{X}\right|} - \left|\boldsymbol{X}\right|\right|,\ p_3 = \sqrt{\Delta v_{threshold}{}^2 - \left|\boldsymbol{X}\right|^2}$$

Therefore, the total cost can be written as

$$\Delta v = \Delta v_1 + \Delta v_{2\min} + \Delta v_3 \tag{14}$$

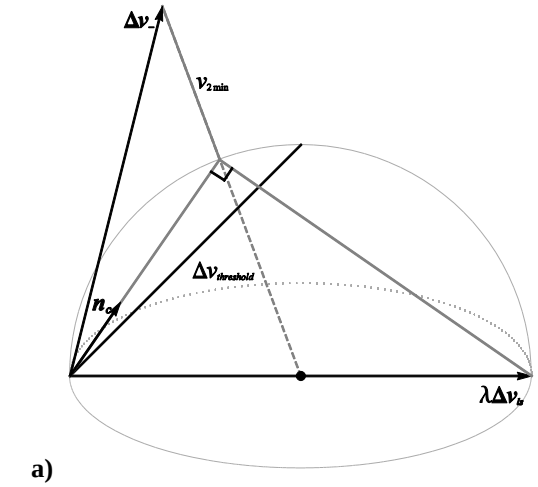

a)

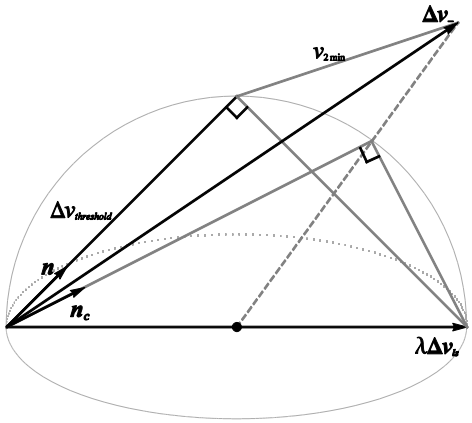

b)

Fig. 6 Geometric relationship of the vectors in Eq. (10) (a) when $\left|\Delta \boldsymbol{v}_{ls}{}^{T} \boldsymbol{n}_c\right| \le \Delta v_{threshold}$ (b) when $\left|\Delta \boldsymbol{v}_{ls}{}^{T} \boldsymbol{n}_c\right| > \Delta v_{threshold}$.

C. Analysis of impact mechanics

The relative kinetic energy E of the large asteroid and the small asteroid at collision can be written as

$$E = \frac{m_l m_s}{2(m_l + m_s)} \Delta v_n{}^2 \tag{15}$$

Assuming that the large and small asteroid have the same composition, the relative kinetic energy is partitioned in equal parts between the two asteroids [34]. If the small asteroid is shattered, the size of the largest fragment as a fraction of the original mass is given by [35, 36]

$$f_l = \frac{1}{2}\left(\frac{S_s m_s}{\rho E/2}\right)^{1.24} \tag{16}$$

The effective impact strength of the small asteroid S_s can be written as [37, 38]

$$S_s = S_{s0} + \frac{\pi k G \rho D^2}{15} \tag{17}$$

The model of the impact strength in Eq. (17) consists of two components: the first part is related to the material properties of the small asteroid and the second part is due to its self-compressional strength. For asteroids with diameters less than approximately 10 km, the compressive strength can be ignored compared to the material strength so that $S_s \approx S_{s0}$ [38].

If the small asteroid remains intact after collision, $f_l = 1$ and thus the threshold of the Δv_n can be can be estimated as

$$\Delta v_{threshold} = 2\sqrt{\frac{S_s(m_l + m_s)}{\kappa \rho m_l}} \approx 2\sqrt{\frac{S_s}{\kappa \rho}} \tag{18}$$

where $\kappa = 2^{1/1.24}$. There are a range of experimental studies using small projectiles to impact large targets with the results for the ratio of the mass of the largest fragment to the initial target mass, as a function of impact strength or the impact energy. Since the material properties of the target asteroids are largely unknown, we simply consider two special cases: metallic asteroids and the basalt asteroids. From [37], it can be shown that $S_{s0} = 1\times10^8$ J/m^3 and $\rho = 6000$ kg/m^3 for metallic asteroids and $S_{s0} = 3\times10^6$ J/m^3 and $\rho = 3000$ kg/m^3 for basalt asteroids. Therefore, we can obtain $\Delta v_{threshold} \approx 196$ m/s for metallic asteroids and $\Delta v_{threshold} \approx 48$ m/s for basalt asteroids. In fact, capturing a fragment of an asteroid is also of interest and so the value of $\Delta v_{threshold}$ would in principle be much larger than that stated above if $f_l < 1$. In practice however, due to the assumptions and uncertainties stated above, active protection (e.g. an ablative layer or air-bags) for the target small asteroid could in principle be required. Although clearly speculative, the use of active protection would have the potential to increase $\Delta v_{threshold}$. For example, the spacecraft could be assumed to carry an ablative coating or air-bags. After it deflects the target small asteroid from its initial orbit to transfer to the large asteroid, the ablative materials or air-bags could be installed by the spacecraft on the surface of the small asteroid where the collision of the two asteroids will occur. Once such active protection is

installed, the ablative material or airbags could sacrificially protect the small asteroid form disruption. Clearly this would incur significant technical challenges which are not addressed here.

D. Selection of candidate large asteroids

In previous work [2, 6], it is shown that the small asteroid can be captured onto periodic orbits at the Sun-Earth L_1 or L_2 points in a direct capture strategy by solving the Lambert arc problem between the small asteroid's initial orbit and the stable manifold associated with the periodic orbits at the Sun-Earth L_1 or L_2 points. In the direct capture strategy, the candidate asteroid is first assumed to leave its orbit with an initial maneuver and will then move onto the stable manifold of the Sun-Earth L_1/L_2 periodic orbit with a second maneuver. These two maneuvers can be calculated by solving a Lambert arc between the asteroid orbit and the stable manifold in the Sun-centered two-body problem. Finally, once the asteroid moves onto the stable manifold, it will then transfer to the target periodic orbit without any further maneuvers.

In this prior direct capture problem, there are 5 variables and optimal strategies for direct capture can be obtained by optimizing these variables. The optimal total cost of the direct capture strategy is denoted as ΔV. Here we expect to capture the small asteroid by impacting the large asteroid with the total cost being lower than ΔV. In order to find low energy capture trajectories for the small asteroid, we set $\Delta V/2$ as the threshold of the first impulse Δv_1 and thus this critical value can be utilized as a selection criterion for the large asteroid. For the small asteroid, the Lambert transfer between the small asteroid and the large asteroid can then be optimized using sequential quadratic programming (SQP), implemented in MATLAB's function *fmincon*. Single objective optimizations with the first impulse Δv_1 as a cost function can then be carried out. For one given target small asteroid, there are 2 variables in the solution vector of this optimization problem: T_0 and T_{fly1}. Their bounds can be obtained through the procedure in Section III.B. An example of large asteroids selected when considering the capture of the small asteroid 2008JL24 is shown in Fig. 7 for illustration.

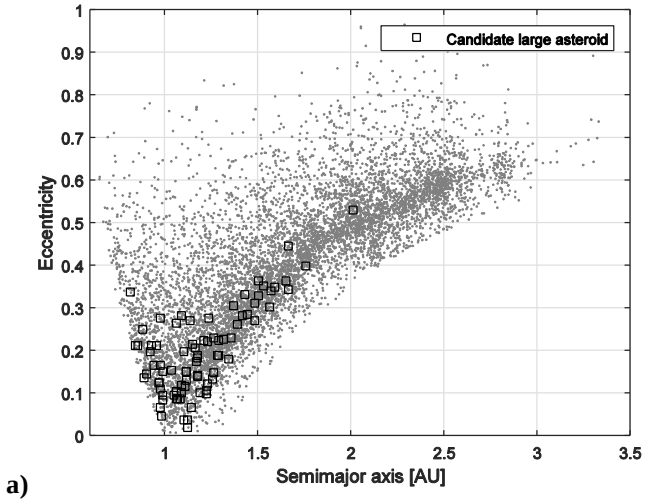

a)

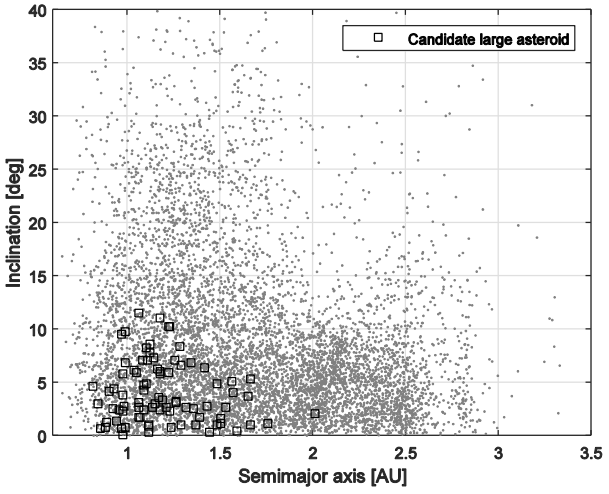

b)

Fig. 7 Candidate large asteroids when capturing 2008JL24 with $\Delta V/2$=475.3 m/s.

E. Design procedure and optimization

The design procedure is now as follows: one candidate small asteroid with H > 25.33 (e.g. 2008JL24) is first selected and then the corresponding candidate large asteroids can be found using the selection criteria in Section IV.D, as shown in Fig. 7. Thus, one target large asteroid in Fig. 7 (e.g. 2001QJ142) is selected. Then given the deflection date T_0 and the first flight time T_{fly1} ($T_0 \in [2020, T_s]$, $T_0 + T_{fly1} \in [2020, T_l]$), the trajectory from the candidate small asteroid orbit to the large asteroid can be calculated as the heliocentric Lambert arc of a two-body problem. Thus, the first impulse Δv_1 can then be obtained. Given the Jacobi constant J, t_p and t_m, the stable manifold associated with the target periodic orbit can then be calculated. Given the second flight time T_{fly2}, the transfer trajectory from the vicinity of the large asteroid to the stable manifold is designed by solving the Lambert arc and so

the third impulse Δv_3 can be obtained. The second impulse Δv_2 can then be optimized by using Eq. (12) and Eq. (13) and the entire transfer trajectory from the small asteroid orbit to the stable manifold can be designed, shown in Fig. 8.

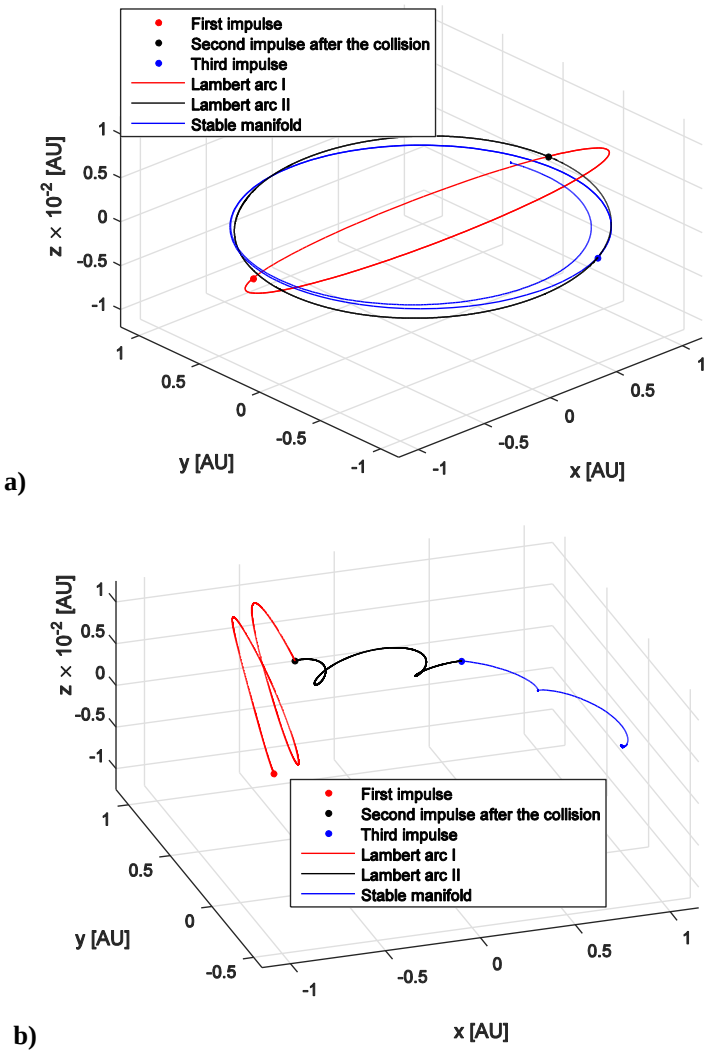

Fig. 8 Transfer trajectory for capturing 2008JL24 by impacting 2001QJ142 (a) in the Sun-centered inertial frame; (b) in the Sun-Earth rotating frame, assuming that they are metallic asteroids.

Table 1 Results for the capture of metallic asteroids with and without impacting large metallic asteroids

Small asteroid	Large asteroid	Total cost using impact, m/s	Flight time using impact, day	Total cost without impact, m/s	Flight time without impact, day	Final target orbit
2006JY26	2002VX91	1021.1	2753.1	1234.2	1997.4	L_1
2008KT	2002VX91	1269.4	2378.2	1454.5	2041.9	L_1
2009BD	2000SG344	431.0	2001.5	602.8	1848.0	L_1
2009BD	2007CS5	394.2	2510.2	602.8	1848.0	L_1
2011UD21	2002VX91	363.9	2610.2	678.7	2037.6	L_1
2013RZ53	2016FZ12	978.3	2620.7	1193.1	1321.1	L_1
2014HN2	2010VC72	987.9	1485.8	1344.0	1600.1	L_1
2008HU4	2012DK4	618.0	1864.1	795.9	2112.5	L_2
2008HU4	2003LN6	359.0	2630.1	795.9	2112.5	L_2
2008HU4	2010JK1	579.1	2548.6	795.9	2112.5	L_2
2008JL24	2001QJ142	780.4	1418.9	950.7	1996.9	L_2
2008JL24	2011MW1	767.4	1692.8	950.7	1996.9	L_2
2008JL24	2016CF137	648.3	1565.8	950.7	1996.9	L_2
2010VQ98	2016ST2	698.8	2215.7	772.6	1905.2	L_2
2010VQ98	2016TP11	653.4	2539.7	772.6	1905.2	L_2
2011MD	2015XP128	1126.8	1982.2	1270.8	1775.6	L_2
2012EP10	1999SF10	1131.1	2209.8	1302.2	1960.5	L_2
2012EP10	2004XK3	1213.4	2235.0	1302.2	1960.5	L_2
2012TF79	2012DK4	337.0	2022.4	546.2	1799.7	L_2
2012TF79	2014NZ64	362.0	2363.9	546.2	1799.7	L_2
2012WR10	2014KF39	777.8	1407.8	948.9	1739.2	L_2
2012WR10	2015VO105	756.5	1365.2	948.9	1739.2	L_2
2013RZ53	2013BS45	977.4	2459.5	1193.1	1321.1	L_2
2014WX202	2012FC71	231.8	2006.8	413.4	1699.5	L_2
2014WX202	2011BP40	358.2	2604.7	413.4	1699.5	L_2
2014WA366	2003SM84	981.0	2348.3	1035.6	1634.3	L_2
2015JD3	2015XA352	1297.3	1585.9	1415.7	1979.3	L_2
2015KK57	2012MD7	549.0	1771.3	667.4	2053.3	L_2
2015VC2	2009TP	347.5	2652.1	706.0	2017.7	L_2

Table 2 Results for the capture of basalt asteroids with and without impacting large basalt asteroids

Small asteroid	Large asteroid	Total cost using impact, m/s	Flight time using impact, day	Total cost without impact, m/s	Flight time without impact, day	Final target orbit
2006JY26	2002VX91	1336.6	2645.5	1234.2	1997.4	L_1
2008KT	2002VX91	1606.9	2682.6	1454.5	2041.9	L_1
2009BD	2000SG344	531.6	2902.4	602.8	1848.0	L_1
2009BD	2007CS5	701.9	2375.2	602.8	1848.0	L_1
2011UD21	2002VX91	621.4	1825.0	678.7	2037.6	L_1
2013RZ53	2016FZ12	1249.8	2274.2	1193.1	1321.1	L_1
2014HN2	2010VC72	1293.3	1430.6	1344.0	1600.1	L_1
2008HU4	2012DK4	775.4	1869.5	795.9	2112.5	L_2
2008HU4	2003LN6	669.1	2531.6	795.9	2112.5	L_2
2008HU4	2010JK1	857.6	2502.9	795.9	2112.5	L_2
2008JL24	2001QJ142	948.8	1541.9	950.7	1996.9	L_2
2008JL24	2011MW1	990.2	1747.6	950.7	1996.9	L_2
2008JL24	2016CF137	853.4	1261.8	950.7	1996.9	L_2
2010VQ98	2016ST2	771.4	2125.2	772.6	1905.2	L_2
2010VQ98	2016TP11	1093.8	2151.8	772.6	1905.2	L_2
2011MD	2015XP128	1240.4	2225.8	1270.8	1775.6	L_2
2012EP10	1999SF10	1423.9	2173.9	1302.2	1960.5	L_2
2012EP10	2004XK3	1421.0	2324.9	1302.2	1960.5	L_2
2012TF79	2012DK4	493.2	2529.1	546.2	1799.7	L_2
2012TF79	2014NZ64	496.0	2512.9	546.2	1799.7	L_2
2012WR10	2014KF39	890.9	1384.2	948.9	1739.2	L_2
2012WR10	2015VO105	946.6	1765.9	948.9	1739.2	L_2
2013RZ53	2013BS45	1116.8	2804.9	1193.1	1321.1	L_2
2014WX202	2012FC71	443.0	1572.2	413.4	1699.5	L_2
2014WX202	2011BP40	408.0	2599.6	413.4	1699.5	L_2
2014WA366	2003SM84	1008.7	2348.9	1035.6	1634.3	L_2
2015JD3	2015XA352	1414.4	2417.3	1415.7	1979.3	L_2
2015KK57	2012MD7	704.3	2174.7	667.4	2053.3	L_2
2015VC2	2009TP	640.3	2680.8	706.0	2017.7	L_2

According to the design procedure stated above, the transfer trajectory from the small asteroid's initial orbit to the stable manifold can be designed and then the 6 variables can be optimized using NSGA-II, a global optimization method that uses a non-dominated sorting genetic algorithm [39]. In order to limit the total duration of the transfers,

the Lambert arcs needed for designing the transfer from the small asteroid's orbit to the large asteroid and the transfer from the large asteroid's orbit to the stable manifolds are assumed to be up to 2 complete revolutions. The optimal results of small asteroid capture by impacting large asteroids are shown in Table 1 and Table 2, corresponding to metallic asteroids and basalt asteroids, respectively. For comparison, the direct capture of small asteroids onto bound periodic orbits around the Sun-Earth L_1 and L_2 points without impact can be designed directly from the asteroid orbit to the stable manifolds. The optimal results are also shown in Table 1 and Table 2.

By comparison of the results with and without impacting the large asteroid in Table 1, it can be seen that the capture of small asteroids by impacting large asteroids has the potential to reduce energy, especially for cases such as 2009BD, 2011UD21 and 2015VC2. Moreover, a range of large asteroids may be available when capturing the same small asteroid, e.g. when capturing 2008JL24. Furthermore, one small asteroid can be captured onto periodic orbits around either the Sun-Earth L_1 or L_2 points by impacting different large asteroids, e.g. 2013RZ53. This implies that the impact can increase the range of capture opportunities. However, due to the additional transfer time from the small asteroid orbit to the large asteroid orbit, the capture of the small asteroid using a large impacting asteroid always needs more flight time than a direct capture.

In this capture strategy, the collision of the small asteroid and large asteroid provides an impulsive maneuver for the small asteroid and it is the mechanics of this interaction that reduces the energy required for the capture strategy. Therefore, the total cost of the capture strategy greatly depends on the threshold of the maneuver which is provided by the collision, while avoiding fragmentation of the asteroid. Furthermore, comparing the results in Table 1 and Table 2, we can note that a smaller value of $\Delta v_{threshold}$ can lead to an increase of the total cost. Moreover, with a smaller value of $\Delta v_{threshold}$, the total cost of capturing some asteroids by impacting large asteroids can be even more than the direct capture strategy, e.g. 2008KT, 2012EP10 and 2015KK57. This is one drawback of the capture strategy of using a small asteroid to impact a large asteroid, since many of the small asteroids are thought to be rubble piles and thus the collision between these asteroids can only provide a limited maneuver. However, through the analysis in Section IV.C, if we capture one segment of an asteroid, not the entire asteroid, the collision can in principle deliver a much larger impulse. Moreover, the use of active protection (e.g. air bags) could in principle increase the value of $\Delta v_{threshold}$.

One of the challenges of this capture strategy is the uncertainty of the properties of the candidate asteroids, including their shape, mass and material properties. Therefore, pre-launch observations using the radar and

optical/infrared telescopes are required to provide good estimates of these parameters [40, 41]. Moreover, in-situ asteroid exploration missions, including the flyby and rendezvous, can also be viewed as an effective way to address these uncertainties [42]. An accurate navigation and control strategy would be also required to guarantee that the candidate small asteroid impacts the large asteroid with the correct collision geometry to achieve the required maneuver for asteroid capture.

V. Small asteroid capture by tether-assisted flyby of large asteroids

Another momentum exchange strategy to transfer small asteroids onto the stable manifold associated with the Sun-Earth L_1 or L_2 points is to use a tethered assist. In this capture strategy, the small asteroid approaches the large asteroid and then connects to the large asteroid through a tether, such that the tether is released after the flyby. Again, the small asteroid will be transferred onto the stable manifold associated with the Sun-Earth L_1 or L_2 points.

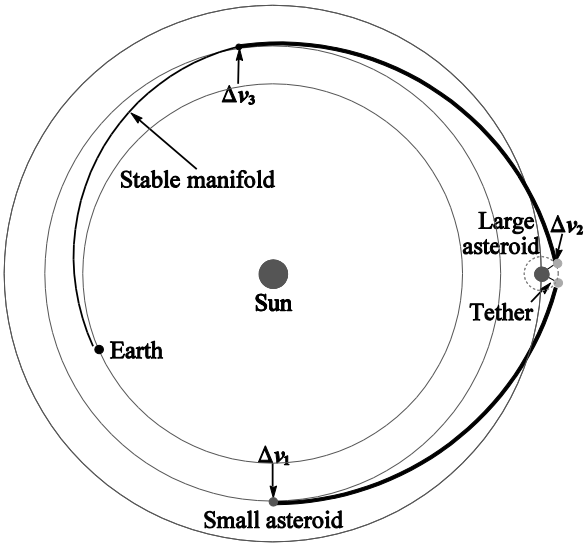

Fig. 9 Overview of small asteroid capture using tether-assisted fly-by.

A. Statement of the problem

A schematic of the tether-assist strategy is shown in Fig. 9. The mission scenario consists of the following steps: with the first impulse $\Delta \boldsymbol{v}_1$, the small asteroid leaves its initial orbit and will then approach the target large asteroid; the small asteroid connects to the large asteroid by a tether until it is released so that the second impulse $\Delta \boldsymbol{v}_2$ is added; with the third impulse $\Delta \boldsymbol{v}_3$, the small asteroid is captured onto the stable manifold associated with the Sun-Earth L_1 or L_2 points.

For this strategy, given one small asteroid and one large asteroid, there are now 7 variables in the problem: the date (T_0) of the first impulse $\Delta \boldsymbol{v}_1$, the flight time (T_{fly1}) of the small asteroid to reach the vicinity of the large asteroid, the tether connection time (T_{tether}), the flight time (T_{fly2}) of the small asteroid between the moment when the small asteroid is released and the moment when the small asteroid injects onto the stable manifold, the Jacobi constant (J) of the target periodic orbit around the Sun-Earth L_1 or L_2 point, the parameter (t_p) determining the point on the periodic orbit where the stable manifold is calculated from, and the stable manifold transfer time (t_m) which determines the point on the stable manifold where the small asteroid inserts onto it. It should be noted that if the connection of the two asteroids is instantaneous and thus $T_{tether} \approx 0$, then there are only 6 variables required to define the problem.

B. Dynamical model during tether-assisted fly-by

In this problem, it is assumed that a spacecraft is first launched and then achieves a rendezvous with each asteroid to prepare an anchor point using a penetrator or a surrounding net or bag [17]. As the small asteroid approaches the vicinity of the large asteroid, the two anchor points are assumed to be connected by a tether. The spacecraft-asteroid tether attachment is assumed to occur when the velocity vector is exactly perpendicular to the radius vector between the two asteroids. Therefore, high-precision navigation is clearly required, but again will not be considered here.

Since the mass ratio of the two asteroids is large (Eq. (6)), here we assume that the large asteroid's orbit during the small asteroid fly-by is unchanged. Before the flyby, the relative velocity of the small asteroid with respect to the large asteroid can therefore be written as

$$\Delta \boldsymbol{v}_{sl} = \boldsymbol{v}_{s-} - \boldsymbol{v}_{l-} \tag{19}$$

Considering the relative velocity $\Delta \boldsymbol{v}_{release}$ of the small asteroid with respect to the large asteroid when released, we have

$$\left|\Delta \boldsymbol{v}_{sl}\right| = \left|\Delta \boldsymbol{v}_{release}\right| \tag{20}$$

and so the velocity vector of the small asteroid after the flyby can be written as

$$\boldsymbol{v}_{s+} = \boldsymbol{v}_{l-} + \Delta \boldsymbol{v}_{release} \tag{21}$$

Moreover, $\boldsymbol{v}_{Lam}$ is again the velocity vector of the small asteroid required for the Lambert arc to the stable manifold after the fly-by, the second impulse can therefore be written as

$$\Delta\boldsymbol{v}_2 = \boldsymbol{v}_{Lam} - \boldsymbol{v}_{s+} = \Delta\boldsymbol{v}_- - \Delta\boldsymbol{v}_{release} \tag{22}$$

where

$$\Delta\boldsymbol{v}_- = \boldsymbol{v}_{Lam} - \boldsymbol{v}_{l-} \tag{23}$$

The minimum value of the second impulse is then found to be

$$\Delta v_{2\min} = \min(|\Delta\boldsymbol{v}_2|) = \min(|\Delta\boldsymbol{v}_- - \Delta\boldsymbol{v}_{release}|) = \big||\Delta\boldsymbol{v}_-| - |\Delta\boldsymbol{v}_{ls}|\big| \tag{24}$$

when $\Delta\boldsymbol{v}_{release}$ has the same direction as $\Delta\boldsymbol{v}_-$. Therefore, the total cost can be written as

$$\Delta v = \Delta v_1 + \Delta v_{2\min} + \Delta v_3 \tag{25}$$

C. Analysis of the tether forces

When the small asteroid connects to the large asteroid via the tether, the small asteroid has a relative velocity of $\Delta\boldsymbol{v}_{sl} = \boldsymbol{v}_s - \boldsymbol{v}_l$ with respect to the large asteroid. Then, after the tether is connected, the small asteroid moves in a circle around the large asteroid with radius *L*, and so the tether tension at the small asteroid is $T_L = m_s\omega^2 L$, where $\omega = |\Delta\boldsymbol{v}_{sl}| / L$. Thus, the tension *T* can be written as [17]

$$\frac{dT}{dr} = -A\rho_{tether}\omega^2 r \tag{26}$$

where r is the distance along the tether with respect to the large asteroid and $r \in [0, L]$. Considering the boundary condition $T_L = m_s\omega^2 L$ ($r = L$), the solution of Eq. (26) is given by

$$T = m_s\omega^2 L + \frac{1}{2}\rho_{tether}\omega^2(L^2 - r^2) \tag{27}$$

Considering that the tether mass is $m_{tether} = \rho_{tether} AL$, the stress on the tether is

$$S = \frac{T}{A} = \left(\frac{m_s}{m_{tether}} + \frac{L^2 - r^2}{2L^2}\right)\rho_{tether}(|\Delta\boldsymbol{v}_{sl}|)^2 \tag{28}$$

Therefore, the maximum tether stress is $S_{\max} = (m_s / m_{tether} + 1/2)\rho_{tether}(|\Delta \boldsymbol{v}_{sl}|)^2$ when $r = 0$. If the maximum safe working stress of the tether is defined as S_0, the small asteroid-to-tether mass ratio can then be written as [17]

$$\frac{m_s}{m_{tether}} = (\frac{v_c}{|\Delta \boldsymbol{v}_{sl}|})^2 - \frac{1}{2} \tag{29}$$

where $v_c = \sqrt{S_0 / \rho_{tether}}$.

It is assumed now that small asteroid-to-tether mass ratio is 20-to-1, i.e., the mass of the smaller asteroid is at least twenty times larger than that of the tether [18]. From Eq. (29), we can note that the characteristic velocity of the tether has a substantial effect on the threshold of $|\Delta \boldsymbol{v}_{sl}|$ and thus two different tether materials will be considered to compare their performance. One is Carbon nanotube tether (CNT) with a density 1300 kg/m^2, a maximum safe working stress of 130 GPa and a characteristic velocity of 10 km/s. This material is chosen from the example of Van Zandt [18]. From Eq. (29), the threshold of the relative velocity of the small asteroid with respect to the large asteroid is then approximately 2200 m/s. The other material considered is the Zylon tether with a characteristic velocity of 2.7 km/s [43] and so the threshold of the relative velocity of the small asteroid with respect to the large asteroid is then approximately 600 m/s.

D. Selection strategy for candidate asteroids

Here we again suppose that $\Delta V/2$ is the threshold of the magnitude of the first impulse Δv_1. Therefore, the threshold of the first impulse Δv_1 and the threshold of the relative velocity $|\Delta \boldsymbol{v}_{sl}|$ between the two asteroids when they approach can be utilized as the selection criteria for the large asteroid. For the small asteroid, the Lambert transfer to the large asteroid can again be optimized using SQP. Single objective optimizations with the first impulse Δv_1 as a cost function can then be carried out. There are again 2 variables in the optimization problem: T_0 and T_{fly1}. Their search domains are assumed to be $T_0 \in [2020, T_s]$ and $T_0 + T_{fly1} \in [2020, T_l]$.

E. Design procedure and optimization

The design procedure is as follows: one candidate small asteroid with H > 25.33 (e.g. 2008JL24) is first selected. Then the set of the candidate large asteroids can be obtained using the selection criteria in Section V.D and thus one target large asteroid is selected. Given the deflection date T_0 and the first flight time T_{fly1}

($T_0 \in [2020, T_s]$, $T_0 + T_{fly1} \in [2020, T_l]$), the trajectory from the candidate small asteroid orbit to the large asteroid can again be calculated as the heliocentric Lambert arc of a two-body problem (Lambert arc I), and thus the first impulse can then be obtained. Then the small asteroid connects to the large asteroid via the tether until it is released. Given the Jacobi constant J, t_p and t_m, the stable manifold associated with the target periodic orbit can be calculated. Given the flight time T_{fly2}, the transfer trajectory from the vicinity of large asteroid to the stable manifold is designed by solving a Lambert arc (Lambert arc II) and so the third impulse can be obtained. The second impulse can then be optimized by using the Eq. (24) and so the entire transfer trajectory can be designed, as shown in Fig. 10.

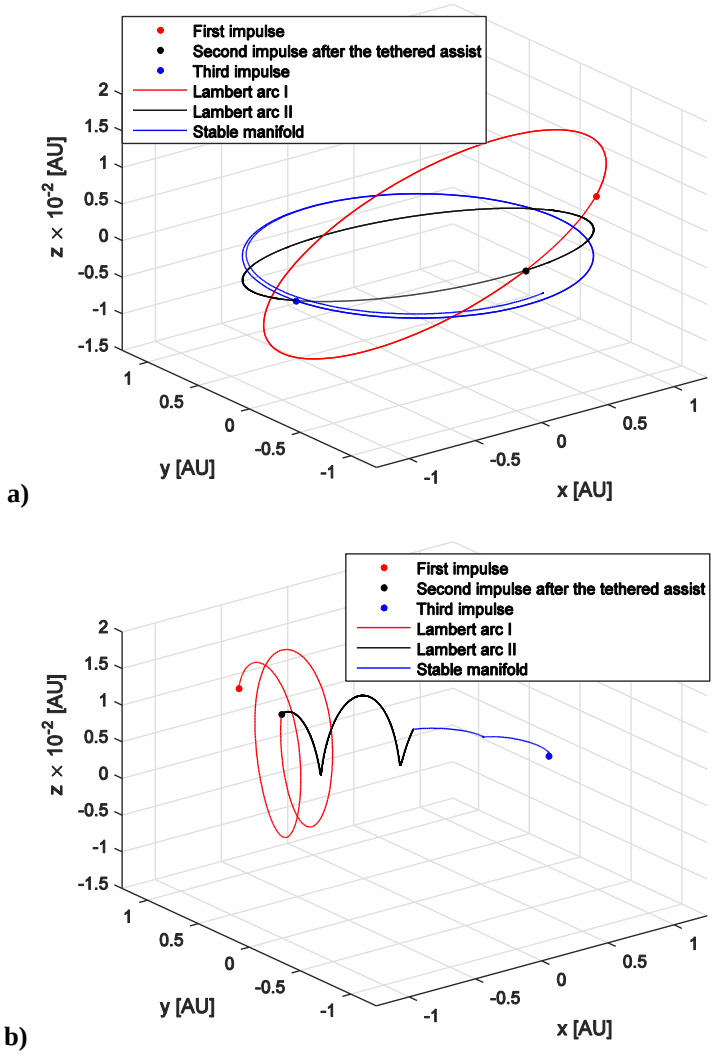

Fig. 10 Transfer trajectory for capturing 2008JL24 using the Carbon nanotube tethered flyby of 2015KE (a) in the Sun-centered inertial frame; (b) in the Sun-Earth rotating frame.

Table 3 Results for asteroid capture with and without the Carbon nanotube tether assist

Small asteroid	Large asteroid	Total cost using impact, m/s	Flight time using impact, day	Total cost without impact, m/s	Flight time without impact, day	Final target orbit
2008JL24	2000SG344	578.3	1992.7	950.7	1996.9	L_1
2008WO2	2010JK1	919.3	2505.9	2805.2	1808.4	L_1
2009BD	2000SG344	248.31	2007.3	602.8	1848.0	L_1
2009SH1	2016FP12	1832.9	2209.6	4125.8	2023.7	L_1
2010TE55	2000SG344	320.7	3082.1	1604.6	1429.6	L_1
2012EP10	2000SG344	886.7	2109.3	1302.2	1960.5	L_1
2014HJ197	2000SG344	531.0	2436.1	2040.4	2185.5	L_1
2014HJ197	2015KE	601.3	2835.3	2040.4	2185.5	L_1
2014HY198	2006HE2	816.4	2529.0	3055.9	1887.1	L_1
2014WU200	2000SG344	628.2	1978.6	849.1	1540.7	L_1
2015VU64	2007VU6	509.4	3227.0	1796.8	1570.3	L_1
2015VU64	2015BM510	1068.6	1876.0	1796.8	1570.3	L_1
2015TC25	2000SG344	418.8	2808.1	2494.3	2089.7	L_1
2016ES85	2007VU6	1154.2	1673.9	1468.5	1543.3	L_1
2008JL24	2015KE	411.2	2259.6	950.7	1996.9	L_2
2008WO2	2010JK1	1216.0	1636.4	2805.2	1808.4	L_2
2012EP10	2016CF137	565.5	2384.4	1302.2	1960.5	L_2
2012HN1	2003SM84	833.2	2205.6	2417.8	2151.5	L_2
2012XB112	2014YD	1852.4	2985.7	1903.3	2178.2	L_2
2013RZ53	2016RD34	559.0	3386.6	1193.1	1321.1	L_2
2013PG10	2009CV	1287.5	2976.4	2613.2	2146.1	L_2
2014HJ197	2015KE	1151.4	2399.3	2040.4	2185.5	L_2
2014HJ197	2016UE	1181.0	2864.1	2040.4	2185.5	L_2
2014HY198	2003SM84	1671.5	1512.4	3055.9	1887.1	L_2
2015HM182	2016TB18	1012.5	2749.6	3254.5	1969.8	L_2
2015ON22	2012EC	669.6	2283.8	2201.2	1869.7	L_2
2015VU64	2007VU6	545.6	2289.4	1796.8	1570.3	L_2
2016ES85	2014QN266	280.5	2421.5	1468.5	1543.3	L_2
2016GC134	2003SM84	1509.6	3239.8	3120.3	1915.3	L_2

Table 4 Results for asteroid capture with and without the Zylon tether assist

Small asteroid	Large asteroid	Total cost using impact, m/s	Flight time using impact, day	Total cost without impact, m/s	Flight time without impact, day	Final target orbit
2008WO2	2010JK1	2527.3	2241.6	2805.2	1808.4	L_1
2009SH1	2016FP12	3653.9	1998.3	4125.8	2023.7	L_1
2010TE55	2000SG344	1210.9	2175.8	1604.6	1429.6	L_1
2012EP10	2000SG344	1194.5	2256.0	1302.2	1960.5	L_1
2014HJ197	2000SG344	1775.9	2075.2	2040.4	2185.5	L_1
2014HJ197	2015KE	1122.0	2581.2	2040.4	2185.5	L_1
2014HY198	2006HE2	2193.7	4159.8	3055.9	1887.1	L_1
2014WU200	2000SG344	610.0	2022.4	849.1	1540.7	L_1
2015VU64	2015BM510	1585.4	2070.3	1796.8	1570.3	L_1
2015VU64	2007VU6	1139.5	3435.1	1796.8	1570.3	L_1
2015TC25	2000SG344	1996.3	1768.8	2494.3	2089.7	L_1
2016ES85	2007VU6	1454.4	1472.2	1468.5	1543.3	L_1
2008WO2	2010JK1	1880.5	1982.4	2805.2	1808.4	L_2
2012XB112	2014YD	1860.4	2938.6	1903.3	2178.2	L_2
2013RZ53	2016RD34	939.8	3065.7	1193.1	1321.1	L_2
2013PG10	2009CV	2264.1	2159.6	2613.2	2146.1	L_2
2014HJ197	2015KE	1518.7	3365.1	2040.4	2185.5	L_2
2014HJ197	2016UE	1789.8	2954.0	2040.4	2185.5	L_2
2014HY198	2003SM84	2564.2	2546.0	3055.9	1887.1	L_2
2015HM182	2016TB18	2692.0	2652.3	3254.5	1969.8	L_2
2015ON22	2012EC	1799.5	2531.0	2201.2	1869.7	L_2
2015VU64	2007VU6	1312.3	3037.2	1796.8	1570.3	L_2
2016GC134	2003SM84	2434.4	3190.3	3120.3	1915.3	L_2

According to the design procedure detailed above, the transfer trajectory from the small asteroid's initial orbit to the stable manifold is again optimized by NSGA-II. Similarly, it is also assumed that the Lambert arcs required for designing the transfer from the small asteroid's orbit to the large asteroid, and the transfer from the large asteroid's orbit to the stable manifolds, are assumed to be up to 2 complete revolutions. The comparison of the results of asteroid capture with and without the tether-assist is shown in Table 3 and Table 4, corresponding to the Carbon nanotube tether and the Zylon tether. As can be seen from Table 3, the use of the Carbon nanotube tether assist can lead to a substantial saving in total cost, compared with capture without the tether-assist. Four small asteroids seem to be particularly suited to the benefits from this strategy; 2008WO2, 2010TE55, 2012HN1 and 2015ON22. The

results for capturing these four asteroids with the Carbon nanotube tether assist show cost savings of order 60%-80%, compared with capture without it. On the other hand, asteroid capture with the Zylon tether assist also has the potential to reduce the total capture cost, as shown in Table 4. However, this saving in total cost incurs a longer flight time. This is mainly due to the extra flight time due to the transfer from the small asteroid orbit to the large asteroid orbit.

Comparing the results of Table 3 and Table 4, we can conclude that the tether material plays a crucial role in this asteroid capture strategy. A higher characteristic velocity means a larger threshold of the relative velocity between the two asteroids and thus larger savings in the total cost of capturing candidate small asteroids. Moreover, since the threshold of the velocity between the two asteroids is utilized as a filter criterion, the higher characteristic velocity allows more candidate large asteroids to be considered when capturing the same small asteroid. Consequently, with a tether assist of higher characteristic velocity, more small asteroids can be captured with a total cost less than that for the direct capture, as shown in Table 3 and Table 4. This is the main limitation of the small asteroid capture strategy using the tether-assist: the Carbon nanotube tether cannot yet be applied to practical engineering problems, however increases of the characteristic velocity of current tether materials can be foreseen [44]. Therefore, with the improvement of the tether materials, the capture of asteroids using tether assist can in principle save energy compared to more direct strategies.

Table 1 and Table 3 show the results of the two asteroid capture strategies investigated in this paper. Comparing the results of the two strategies, we note that the capture strategy using a tethered-assist flyby has the potential to achieve much lower energy capture than the capture strategy using kinetic impacts, e.g. 2008JL24, 2009BD, 2012EP10 and 2013RZ53. Nevertheless, due to the additional filter criteria in the asteroid capture strategy using tether assist, the capture strategy using kinetic impact in principle enables a wider range of candidate large asteroids to capture the same small asteroid, e.g. 2008JL24, 2009BD and 2012EP10.

In this capture strategy, the main challenge is the limitation of the tether material since the efficiency and feasibility of the capture strategy is strongly dependent on the tether material properties. The ratio of tether material strength to weight is of key importance to the performance of the tether. A number of materials have been developed to increase the ratio of material strength to weight and some tether materials, including Spectra and Zylon, with a high strength-to-weight ratio have been proposed for other tether missions, e.g. Mars missions with tether assists [43, 45]. Current research on Carbon nanotubes suggests remarkable potential for tether materials in the future [18,

46]. The shape of the tether also has an influence its performance and it has been demonstrated that a tapered tether can improve performance for tether missions[47]. Moreover, an accurate navigation and control strategy is also required to ensure that the candidate small asteroid connects reliably to the large asteroid by tether.

VI. Conclusion

Momentum exchange has been proposed to efficiently capture small asteroids into periodic orbits around the Sun-Earth L_1 and L_2 points. The results presented show that momentum exchange can achieve more efficient capture of some asteroids relative to direct manifold capture strategies. On the other hand, the flight time for asteroid capture using momentum exchange is longer than that for direct capture. By comparing the results for asteroid capture using kinetic impacts and asteroid capture using a tether assist, it has been shown that the kinetic impact strategy offers more candidate large asteroids when capturing the same small asteroid. However, the use of a high-stress tether assist can lead to a substantial saving in total cost, compared with small asteroid capture suing kinetic impacts. Future improvements in tether materials will produce more attractive results for this strategy.

The methods proposed in this paper are intended to be used as a preliminary analysis of these asteroid capture strategies. The shape, mass and material properties of the candidate asteroids are the major source of uncertainty. Therefore, pre-launch characterization and observation would be required to identify the geometry and composition of the target asteroids, while high precision navigation and orbit control would be required to ensure the correct geometry for momentum exchange, either through an impact or coupling via a tether.

Acknowledgments

Colin R. McInnes acknowledges support from a Royal Society Wolfson Research Merit Award and Minghu Tan acknowledges support from the China Scholarship Council (CSC).

References

[1] Morbidelli, A., Bottke Jr, W., Froeschlé, C., and Michel, P. "Origin and Evolution of Near-Earth Objects," *Asteroids III*. University of Arizona Press, Tucson, 2002, pp. 409-422.

[2] Yárnoz, D. G., Sanchez, J., and McInnes, C. "Easily retrievable objects among the NEO population," *Celestial Mechanics and Dynamical Astronomy* Vol. 116, No. 4, 2013, pp. 367-388.
doi: 10.1007/s10569-013-9495-6

[3] Mingotti, G., Sánchez, J., and McInnes, C. "Combined low-thrust propulsion and invariant manifold trajectories to capture NEOs in the Sun–Earth circular restricted three-body problem," *Celestial Mechanics and Dynamical Astronomy* Vol. 120, No. 3, 2014, pp. 309-336.
doi: 10.1007/s10569-014-9589-9

[4] Sánchez, J. P., and Yárnoz, D. G. "Asteroid retrieval missions enabled by invariant manifold dynamics," *Acta Astronautica* Vol. 127, 2016, pp. 667-677.
doi: 10.1016/j.actaastro.2016.05.034

[5] Brophy, J. R., Friedman, L., and Culick, F. "Asteroid retrieval feasibility." Keck Institute for Space Studies, California Institute of Technology, Jet Propulsion Laboratory, Pasadena, California, 2012.

[6] Mazanek, D. D., Merrill, R. G., Brophy, J. R., and Mueller, R. P. "Asteroid redirect mission concept: a bold approach for utilizing space resources," *Acta Astronautica* Vol. 117, 2015, pp. 163-171.
doi: 10.1016/j.actaastro.2015.06.018

[7] Mingotti, G., Sanchez, J.-P., and McInnes, C. "Low energy, low-thrust capture of near Earth objects in the Sun–Earth and Earth–Moon restricted three-body systems," *SPACE Conferences & Exposition*. AIAA, Washington, 2014.

[8] Urrutxua, H., Scheeres, D. J., Bombardelli, C., Gonzalo, J. L., and Peláez, J. "Temporarily captured asteroids as a pathway to affordable asteroid retrieval missions," *Journal of Guidance, Control, and Dynamics* Vol. 38, No. 11, 2015, pp. 2132-2145.
doi: 10.2514/1.G000885

[9] Levin, E. M., and Levin, E. M. "Dynamic analysis of space tether missions." American Astronomical Society Publication, San Diego, CA, 2007, pp. 11-17.

[10] Tragesser, S. G. "Static formations using momentum exchange between satellites," *Journal of Guidance, Control, and Dynamics* Vol. 32, No. 4, 2009, pp. 1277-1286.
doi: 10.2514/1.40939

[11] Bombardelli, C., Urrutxua, H., Merino, M., Pelaez, J., and Ahedo, E. "The ion beam shepherd: A new concept for asteroid deflection," *Acta Astronautica* Vol. 90, No. 1, 2013, pp. 98-102.
doi: 10.1016/j.actaastro.2012.10.019

[12] Wie, B. "Dynamics and control of gravity tractor spacecraft for asteroid deflection," *Journal of Guidance, Control, and Dynamics* Vol. 31, No. 5, 2008, pp. 1413-1423.

doi: 10.2514/1.32735

[13] McInnes, C. R. "Near Earth object orbit modification using gravitational coupling," *Journal of Guidance Control and Dynamics* Vol. 30, No. 3, 2007, pp. 870-873.
doi: 10.2514/1.25864

[14] McInnes, C. R. "Deflection of near-Earth asteroids by kinetic energy impacts from retrograde orbits," *Planetary and Space Science* Vol. 52, No. 7, 2004, pp. 587-590.
doi: 10.1016/j.pss.2003.12.010

[15] Vasile, M., and Colombo, C. "Optimal impact strategies for asteroid deflection," *Journal of Guidance, Control, and Dynamics* Vol. 31, No. 4, 2008, pp. 858-872.
doi: 10.2514/1.33432

[16] Michel, P., Cheng, A., and Küppers, M. "Asteroid Impact and Deflection Assessment (AIDA) mission: science investigation of a binary system and mitigation test," *European Planetary Science Congress 2015*. Vol. 10, Nantes, France, 2015, pp. 123-124.

[17] Penzo, P. A., and Mayer, H. L. "Tethers and asteroids for artificial gravity assist in the solar system," *Journal of Spacecraft and Rockets* Vol. 23, No. 1, 1986, pp. 79-82.
doi: 10.2514/3.25086

[18] Van Zandt, J. R. "Tethered asteroids," *AIAA SPACE 2013 Conference and Exposition*. AIAA, San Diego, CA, 2013, pp. 1-19.

[19] Canavan, G. H., and Rather, J. "Assessment of current and future technologies," *Proceedings of the Near-Earth Interception Workshop*. 1992, pp. 227-236.

[20] Nazirov, R., and Eismont, N. "Gravitational maneuvers as a way to direct small asteroids to trajectory of a rendezvous with dangerous near-Earth objects," *Cosmic Research* Vol. 48, No. 5, 2010, pp. 479-484.
doi: 10.1134/S0010952510050175

[21] Wagner, S., and Wie, B. "Hybrid Algorithm for Multiple Gravity-Assist and Impulsive Delta-V Maneuvers," *Journal of Guidance, Control, and Dynamics* Vol. 38, No. 11, 2015, pp. 2096-2107.
doi: 10.2514/1.G000874

[22] Chen, Y., Baoyin, H., and Li, J. "Accessibility of main-belt asteroids via gravity assists," *Journal of Guidance, Control, and Dynamics* Vol. 37, No. 2, 2014, pp. 623-632.
doi: 10.2514/1.58935

[23] Prado, A. F. "Using tethered gravity-assisted maneuvers for planetary capture," *Journal of Guidance, Control, and Dynamics* Vol. 38, No. 9, 2015, pp. 1852-1856.

doi: 10.2514/1.G001009

[24] Koon, W. S., Lo, M. W., Marsden, J. E., and Ross, S. D. "Dynamical systems, the three-body problem and space mission design." Springer-Verlag, New York, 2011, pp. 23-35.

[25] Szebehely, V. *Theory of orbit: The restricted problem of three Bodies*. Academic Press, New York, 1967, pp. 7-29.

[26] Davis, K. E., Anderson, R. L., Scheeres, D. J., and Born, G. H. "Optimal transfers between unstable periodic orbits using invariant manifolds," *Celestial Mechanics and Dynamical Astronomy* Vol. 109, No. 3, 2011, pp. 241-264.
doi: 10.1007/s10569-010-9327-x

[27] Davis, K. E., Anderson, R. L., Scheeres, D. J., and Born, G. H. "The use of invariant manifolds for transfers between unstable periodic orbits of different energies," *Celestial Mechanics and Dynamical Astronomy* Vol. 107, No. 4, 2010, pp. 471-485.
doi: 10.1007/s10569-010-9285-3

[28] Richardson, D. L. "Analytic construction of periodic orbits about the collinear points," *Celestial Mechanics* Vol. 22, No. 3, 1980, pp. 241-253.
doi: 10.1007/BF01229511

[29] Yu, Y., and Baoyin, H. "Generating families of 3D periodic orbits about asteroids," *Monthly Notices of the Royal Astronomical Society* Vol. 427, No. 1, 2012, pp. 872-881.
doi: 10.1111/j.1365-2966.2012.21963.x

[30] Henon, M. "New families of periodic orbits in Hill's problem of three bodies," *Celestial Mechanics and Dynamical Astronomy* Vol. 85, No. 3, 2003, pp. 223-246.
doi: 10.1023/A:1022518422926

[31] Chesley, S. R., Chodas, P. W., Milani, A., Valsecchi, G. B., and Yeomans, D. K. "Quantifying the risk posed by potential Earth impacts," *Icarus* Vol. 159, No. 2, 2002, pp. 423-432.
doi: 10.1006/icar.2002.6910

[32] Perna, D., Barucci, M., Drube, L., Falke, A., Fulchignoni, M., Harris, A., and Kanuchova, Z. "A global response roadmap to the asteroid impact threat: the NEOShield perspective," *Planetary and Space Science* Vol. 118, 2015, pp. 311-317.
doi: 10.1016/j.pss.2015.07.006

[33] Rao, A. "Dynamics of particles and rigid bodies: a systematic approach." Cambridge University Press, 2005, pp. 288-298.

[34] Hartmann, W. "Impact strengths and energy partitioning in impacts into finite solid targets," *Lunar and Planetary Science Conference*. Vol. 19, 1988.

[35] Fujiwara, A., Kamimoto, G., and Tsukamoto, A. "Destruction of basaltic bodies by high-velocity impact," *Icarus* Vol. 31, No. 2, 1977, pp. 277-288.

doi: 10.1016/0019-1035(77)90038-0

[36] O'Brien, D. P., and Greenberg, R. "The collisional and dynamical evolution of the main-belt and NEA size distributions," *Icarus* Vol. 178, No. 1, 2005, pp. 179-212.
doi: 10.1016/j.icarus.2005.04.001

[37] Davis, D. R., Chapman, C. R., Weidenschilling, S. J., and Greenberg, R. "Collisional history of asteroids: Evidence from Vesta and the Hirayama families," *Icarus* Vol. 62, No. 1, 1985, pp. 30-53.
doi: 10.1016/0019-1035(85)90170-8

[38] Durda, D. D., and Dermott, S. F. "The collisional evolution of the asteroid belt and its contribution to the zodiacal cloud," *Icarus* Vol. 130, No. 1, 1997, pp. 140-164.
doi: 10.1006/icar.1997.5803

[39] Deb, K., Pratap, A., Agarwal, S., and Meyarivan, T. "A fast and elitist multiobjective genetic algorithm: NSGA-II," *IEEE transactions on evolutionary computation* Vol. 6, No. 2, 2002, pp. 182-197.
doi: 10.1109/4235.996017

[40] Neeley, J., Clark, B., Ockert-Bell, M., Shepard, M., Conklin, J., Cloutis, E., Fornasier, S., and Bus, S. "The composition of M-type asteroids II: Synthesis of spectroscopic and radar observations," *Icarus* Vol. 238, 2014, pp. 37-50.
doi: 10.1016/j.icarus.2014.05.008

[41] Shepard, M. K., Richardson, J., Taylor, P. A., Rodriguez-Ford, L. A., Conrad, A., de Pater, I., Adamkovics, M., de Kleer, K., Males, J. R., and Morzinski, K. M. "Radar observations and shape model of asteroid 16 Psyche," *Icarus* Vol. 281, 2017, pp. 388-403.
doi: 10.1016/j.icarus.2016.08.011

[42] Gao, Y. "Near-Earth asteroid flyby trajectories from the Sun-Earth L2 for Chang'e-2's extended flight," *Acta Mechanica Sinica* Vol. 29, No. 1, 2013, pp. 123-131.
doi: 10.1007/s10409-013-0011-8

[43] Jokic, M. D., and Longuski, J. M. "Artificial gravity and abort scenarios via tethers for human missions to Mars," *Journal of Spacecraft and Rockets* Vol. 42, No. 5, 2005, pp. 883-889.
doi: 10.2514/1.6121

[44] Bangham, M., Lorenzini, E., and Vestal, L. "Tether transportation system study." NASA TP-1998-206959, 1998.

[45] Jokic, M. D., and Longuski, J. M. "Design of tether sling for human transportation systems between Earth and Mars," *Journal of Spacecraft and Rockets* Vol. 41, No. 6, 2004, pp. 1010-1015.
doi: 10.2514/1.2413

[46] Smitherman, D. "Space Elevators, An Advanced Earth-Space Infrastructure for the New Millennium," *NASA CP-2000-210429*. 2000.

[47] Lorenzini, E., Cosmo, M., Kaiser, M., Bangham, M., Vonderwell, D., and Johnson, L. "Mission analysis of spinning systems for transfers from low orbits to geostationary," *Journal of Spacecraft and Rockets* Vol. 37, No. 2, 2000, pp. 165-172.
doi: 10.2514/2.3562